Conformational Substates of the Oxyheme Centers in α and β Subunits of Hemoglobin As Disclosed by EPR and ENDOR Studies of Cryoreduced Protein†

Roman Davydov,‡ Viktoria Kofman,‡ Judith M. Nocek,‡ Robert W. Noble,§ Hilda Hui,§ and Brian M. Hoffman*,‡

Department of Chemistry, Northwestern University, 2145 Sheridan Road, Evanston, Illinois 60208-3113, and Department of Medicine, State University of New York at Buffalo, and Veterans Administration Medical Center, Buffalo, New York 14215

Received December 17, 2003; Revised Manuscript Received March 23, 2004

ABSTRACT: Exposure of frozen solutions of oxyhemoglobin to γ-irradiation at 77 K yields EPR- and ENDOR-active, one-electron-reduced oxyheme centers which retain the conformation of the diamagnetic precursor. EPR spectra have been collected for the centers produced in human HbO_2 and isolated αO_2 and βO_2 chains, as well as $\alpha O_2\beta(Zn)$, $\alpha(Zn)\beta O_2$, and $\alpha O_2\beta(Fe^{3+})$ hybrids, each in frozen buffer and in frozen glasses that form in the presence of glycols and sugars and also in the presence of IHP. These reveal two spectroscopically distinct classes of such ferriheme centers ($g_1 \leq 2.25$), denoted A and B. Averaged over many similar sites, the A-center has a rhombic EPR signal with a *g*-tensor, $\mathbf{g^A} = [2.248(4), 2.146(1), 1.966(1)]$; the B-center exhibits a less anisotropic EPR signal, $\mathbf{g^B} = [2.216(3), 2.118(2), 1.966(1)]$. Early measurement had suggested that, in the cryoreduced HbO_2 tetramer, the two centers corresponded to the two different chains [Symons, M. C. R., and Petersen, R. L. (1978) *Proc. R. Soc. London, Ser. B 201*, 285−300]. However, the present EPR and ENDOR results show that the two signals instead reflect the fact that the parent oxyhemes exist in two major conformational substates and that this is true for *both* αO_2 and βO_2 subunits: $\alpha O_2{}^A$ (minor species) and $\alpha O_2{}^B$ (major species); $\beta O_2{}^A$(major species) and $\beta O_2{}^B$ (minor species). Similar behavior is seen for MbO_2 [Kappl, R., Höhn-Berlage, M., Hüttermann, J., Bartlett, N., and Symons, M. C. R. (1985) *Biochim. Biophys. Acta 827*, 327−343]. The A/B *g*-tensors of αO_2 and βO_2 chains vary little with the environment of the chains, while the relative populations of the substates depend greatly on glycols and IHP. These results suggest a quaternary influence on the oxyheme distal pocket of α chains and that the glycol-induced changes in the substate populations of the R-state HbO_2 tetramer are largely associated with the αO_2 subunit. ^{1}H ENDOR spectra from the distal histidine proton hydrogen-bonded to the peroxo ligand show very different isotropic coupling for the A- and B-centers. Analysis of the spectroscopic data suggests that the A- and B-centers represent different orientations of the oxyheme O_2 ligand relative to the distal histidine. It is likely that the A and B conformational substates in the αO_2 and βO_2 subunits differ not only in their tertiary structures but in their affinities for O_2.

During the past 25 years, numerous studies have shown that oxyheme centers capture mobile electrons generated by ionizing irradiation of solid solutions or crystals at 4−77 K to form two distinct types of ferriheme intermediates with relatively small *g*-anisotropy (*1*−*14*). Both types of center are stable at 77 K and show rhombic low-spin ferriheme EPR[1] spectra with relatively small *g*-anisotropy. One type, characterized by a *g*-tensor with $g_1 \sim 2.3$, is the hydroperoxoferriheme. The other, which is the primary product of reduction, has a distinctly different *g*-tensor with $g_1 \leq 2.25$ and, in consequence, has been assigned as the peroxoferriheme state (*1*−*3*), an assignment which is under continued investigation (*15*). The primary cryoreduction products ($g_1 \leq 2.25$ centers) have spectroscopic properties that are independent of reduction temperature within the range 6−77 K, indicating that they retain the conformation of the oxyferroheme precursor, essentially unaltered (*2*, *5*). Thus a $g_1 \leq 2.25$ cryoreduced oxyheme center provides a sensitive EPR/ENDOR probe of the active site structure of the EPR-silent precursor oxyhemoprotein (*2*, *5*−*7*).

The EPR spectrum of cryoreduced oxyhemoglobin was shown to be a superposition of two $g_1 \leq 2.25$ EPR signals, A and B (*1*−*3*). On the basis of EPR studies of cryoreduced isolated αO_2 and βO_2 chains (*1*, *2*) as well as valency hybrids of HbO_2 (*3*, *11*), the A and B EPR signals were initially assigned to the cryoreduced oxyheme centers in βO_2 and αO_2 subunits, respectively (*1*−*3*). However, in the context of such an assignment it is puzzling that cryoreduced MbO_2 also reveals two different species, a dominant B-like center and an minor A-like center (*2*). ^{1}H ENDOR spectra of cryoreduced MbO_2 and HbO_2 reveal an exchangeable proton with maximum hyperfine coupling of ∼10 MHz, which is assigned to the distal histidine N−H hydrogen-bonded to the peroxo ligand (*2*, *16*).

The EPR spectra and yield of cryoreduced oxyhemoglobin change in the presence of glycol additives (*1*, *2*). The addition

† This work has been supported by the NIH (Grant GM P01588).
* To whom correspondence should be addressed. Phone: 847-491-3104. Fax: 847-491-7713. E-mail: bmh@northwestern.edu.
‡ Northwestern University.
§ State University of New York at Buffalo and Veterans Administration Medical Center.
[1] Abbreviations: Hb, hemoglobin; EPR, electron paramagnetic resonance; ENDOR, electron nuclear double resonance.

10.1021/bi036273z CCC: $27.50
Published on Web 04/29/2004

of 50% glycerol or ethylene glycol to the protein solution, which leads to glass formation upon cooling to 77 K, significantly increases the yield of the peroxoferriheme centers but has a relatively minor effect on the EPR parameters, and thus most experiments were performed in glassy matrices. However, the relative intensity of the B signal decreases dramatically in the presence of 50% ethylene glycol or glycerol. Conversely, for glassy solutions at pH <7 in the presence of IHP the B signal becomes more intense than the A signal (*3*, *9*). The effect of glycols and IHP on the relative intensities of the A and B signals of HbO_2 was interpreted as reflecting an influence on the relative *rates* of reduction of the oxyheme centers in the α and β subunits (*1*, *2*, *9*). However, this explanation is not consistent with the finding (*2*) that the relative yields of peroxoferriheme centers of the HbO_2 tetramer in glassy solutions are independent of the irradiation dose up to 10 Mrad: if the A and B signals arise from the two chain types, their relative intensities must approach unity as complete reduction is approached, but this is contrary to observation.

To explore this inconsistency, we have performed EPR and ENDOR studies on the peroxoferriheme primary cryoreduction products of human HbO_2, isolated αO_2 and βO_2 chains, hemoglobin M-Milwaukee [αO_2, β(Fe(III)] valency hybrids, [Zn,FeO_2] mixed-metal hybrids, and MbO_2, all under a wide range of conditions involving the addition of glycols, sugars, and IHP. We have found that oxy α and β chains, both isolated and in the Hb tetramer, display two major conformational substates of the oxyheme center, denoted A and B, as does MbO_2. This behavior of the oxyheme pocket is analogous to that seen for CO-Hb (*17*−*19*). The A and B substates of the two Hb subunits and Mb have similar spectroscopic characteristics, but the A/B population ratios in the α and β subunits depend on their environment. We further examine the degree to which substate populations are subject to quaternary influences and constraints within the Hb tetramer.

MATERIALS AND METHODS

Materials. Tris, BisTris, MES, glucose, sucrose, trehalose, myoglobin, and inositol hexaphosphoric acid (IHP) were purchased from Sigma. Glycerol and ethylene glycol were purchased from Aldrich. Human HbO_2 was isolated from whole blood as previously described (*20*, *21*). Isolated αO_2 and βO_2 chains and [αO_2,β(Zn)] and [α(Zn),βO_2] hybrids were prepared as described (*21*). Sample purity was tested by HPLC, IEF, and SDS gel electrophoresis. No detectable amounts of hemoglobin were present in the samples of purified α and β chains, meaning that contamination by HbO_2 was less 0.5%. MbO_2 was made by reduction of 5 mM metMb (Sigma) solution in buffer by a few grains of dithionite followed by gel filtration on an O_2-saturated Sephadex G-25 column to remove a trace of dithionite and to oxygenate deoxy-Mb. HbO_2 M-Milwaukee was isolated according to John and Waterman (*22*). Carp HbO_2 was isolated as described (*23*). Bovine and pigeon HbO_2 were prepared from methemoglobin (Sigma) using the procedure of MbO_2.

In all but one instance, discussed shortly, the oxyhemoglobins samples were reduced at 77 K by γ-irradiation with a ^{60}Co source (Gammacell 220) to a dose of ∼3 Mrad as described (*5*, *24*).

X-band EPR spectra were recorded on a modified Varian E-4 spectrometer at 77 K. Q-band (35 GHz) EPR and ENDOR spectra were recorded on a modified Varian E-110 spectrometer equipped with a helium immersion Dewar at 2 K and operating in dispersion mode using 100 kHz field modulation under "rapid passage" conditions (*25*). For ENDOR, in some instances, the radio frequency (RF) bandwidth was broadened to 60−200 kHz to improve the signal-to-noise ratio (*26*). EPR spectra of cryoreduced samples exhibit strong signals from free radicals created by the irradiation; this region is deleted from the spectra shown, for clarity. The EPR signals of cryoreduced HbO_2 were quantitated using a 1 mM solution of $Cu(ClO_4)_2$ as standard.

For a single orientation of a paramagnetic center, the first-order ENDOR spectrum of a nucleus with $I = {}^1/_2$ in a single paramagnetic center consists of a doublet with frequencies given by (*27*)

$$\nu_{\pm} = |\nu_N \pm A/2| \quad (1)$$

Here, ν_N is the nuclear Larmor frequency and A is the orientation-dependent hyperfine coupling constant of the coupled nucleus. The doublet is centered at the Larmor frequency and separated by A when $\nu_N > |A/2|$, as in case for the ^{1}H spectra presented here. The full hyperfine and quadrupole tensors of the coupled nucleus can be obtained by analyzing a "2D" field-frequency set of orientation-selective ENDOR spectra across the EPR envelope, as described elsewhere (*28*−*30*).

RESULTS

Figure 1 presents EPR spectra of cryoreduced HbO_2 in polycrystalline frozen buffer and in frozen glasses formed by the addition of glycerol (gly) and ethylene glycol (EG), as well as the sugars glucose, sucrose, and trehalose. Addition of all the polyols and sugars increases the yield of the radiolytic cryoreduction of HbO_2 by a factor of 2−4 (not shown), consistent with other observations (*31*). As previously reported (*1*, *2*), the EPR spectra of cryoreduced HbO_2 in frozen aqueous buffer are a superposition of spectra with roughly equal intensity from two peroxoferriheme centers, A and B, arising from two distinct structures for the parent oxyferroheme centers. Figure 2 presents the corresponding spectra for αO_2 and βO_2 chains, as well as MbO_2; Figure 3 presents the spectra for Hb hybrids. Table S1 presents the individual *g*-tensors for the 14 A-centers and 11 B-centers in the cryoreduced proteins discussed in this work; Table 1 presents the average of tensors for the two classes; the overall spread in *g*-values of ca. ±0.007 is large enough that one can reliably and reproducibly measure differences in *g*-values among members of each class (Table S1). Table 1 includes the analysis of the A and B *g*-tensors in terms of conventional crystal-field parameters that describe the single odd electron in a $t_{2g}(d\pi)$ orbital of a low-spin d^5 configuration on Fe. These are the splitting of the two $d\pi$ (d_{zy}/d_{yz}) orbitals, δ, and the splitting between the odd-electron (highest lying) $d\pi$ orbital and the lowest lying, d_{xy}, orbital, Δ, expressed as ratios to the spin−orbit-coupling parameter, δ/λ, Δ/λ; the third parameter, k, decreases from unity with increasing covalency with ligands.

HbO_2 Tetramer. The B component of the ca. 1/1 A/B superposition seen for HbO_2 in frozen buffer (Figure 1A) is

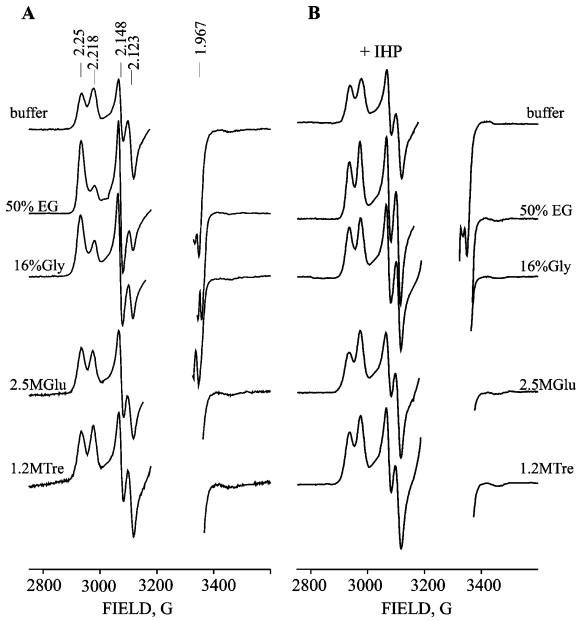

FIGURE 1: X-band EPR spectra of cryoreduced HbO_2 A in frozen buffer and in the presence of 50% (v/v) ethylene glycol (EG), 16% and 2.5% (v/v) glycerol (Gly), 2.5 M glucose (Glu), and 1.2 M trehalose (Tre) in the absence (panel A) and the presence of IHP (panel B). Conditions: 3 mM HbO_2 (in heme) and 50 mM BisTris, pH 6. Instrument settings: 77 K, 100 kHz modulation frequency, 5 G modulation amplitude, 9.15 GHz microwave frequency, and 2 mW microwave power.

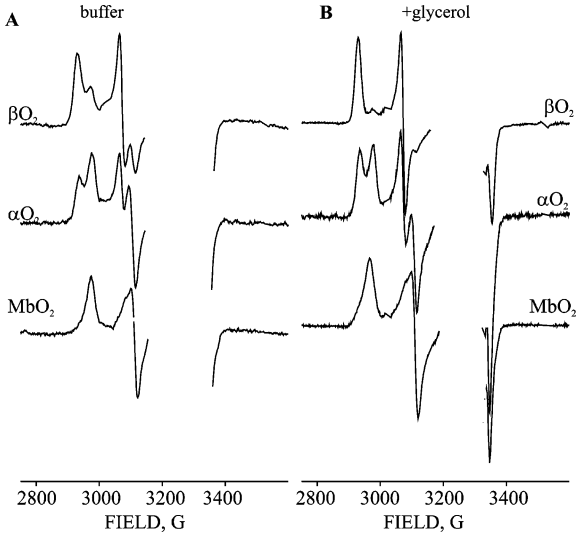

FIGURE 2: X-band EPR spectra of cryoreduced isolated αO_2 and βO_2 chains and MbO_2 in frozen buffer (panel A) and in the presence of 16% glycerol (panel B). Conditions: 50 mM BisTris, pH 7. Instrument settings as in Figure 1.

Table 1: Average *g*-Values in A and B Substates of Cryoreduced $[FeO_2]^7$ Centers in HbO_2, Chains, and Hybrids[a]

substate	g_1	g_2	g_3
A[b]	2.248(4)	2.146(1)	1.966(1)
B[c]	2.216(3)	2.118(2)	1.966(1)

[a] Average values (standard deviations) for the 14 A-centers and 11 B-centers of Table S1. [b] Crystal-field parameters: $\delta/\lambda = 7.5$, $\Delta/\lambda = 11.6$, and $k = 0.80$. [c] Crystal-field parameters: $\delta/\lambda = 7.8$, $\Delta/\lambda = 11.8$, and $k = 0.95$.

strongly suppressed by the presence of 50% ethylene glycol or glycerol (Figure 1B); the effect, which is observed for as little as 2.5% glycerol (not shown), slightly diminishes upon increasing the pH from 6.0 to 7.6. In addition, in the presence of glycols, there is a small but reproducible shift of g_1 (Table S1). In contrast, the addition of sugars does not alter the A/B ratio (Figure 1), suggesting that ethylene glycol and glycerol do not simply influence the A/B population in cryoreduced HbO_2 by reducing the activity of water.

The addition of the heterotropic allosteric effector IHP causes negligible changes in the EPR spectra of cryoreduced HbO_2 in frozen buffer (Figure 1B). However, IHP largely stabilizes the oxyheme centers against the perturbing action of glycols, such that the A/B ratio remains (very) roughly 1:1 when they are added in the presence of IHP. As a result, *it appears* that IHP causes a large change in ratio when added to HbO_2 in the presence of glycols, whereas the real perturbation is that caused by the addition of glycols to HbO_2 in buffer. In contrast, it appears that IHP introduces a sensitivity to the addition of sugars (Figure 1B).

To confirm that the cryoreduced oxyheme units do not undergo noticeable conformational changes after reduction at 77 K, a sample of HbO_2 was irradiated for 10−20 min at 6 K in an EPR resonator attached to an electron accelerator, and its EPR spectrum was promptly recorded at this temperature, as described elsewhere (*5*). There are *no* significant differences between the EPR spectra of HbO_2 cryoreduced and examined promptly at 6 K and those of samples irradiated at 77 K, confirming a previous report (*2*). We also find that the EPR spectra of cryoreduced HbO_2 do not change during storage at 77 K for 3 years.

We examined the radiation dose dependence of the ratio of A and B signal intensities for HbO_2 in 50% ethylene glycol/buffer mixture at pH 6, both in the absence and in the presence of IHP, and found in both cases the ratio to be independent of the dose up to 12 Mrad, where 75% ± 10% of all oxyheme centers have been reduced. This result is consistent with previous observation (*2*). However, it is incompatible with the assignment of the A and B signals in these samples to different subunits (*1*, *10*): such an assignment would require that the A/B ratio approach unity with increasing reduction. Instead, the observations indicate that there are two structurally different oxyheme substates *within each subunit*, $\alpha O_2{}^A$,$\alpha O_2{}^B$ and $\beta O_2{}^A$,$\beta O_2{}^B$, that these lead to the A- and B-type EPR signals upon cryoreduction. The effect of cosolvents and IHP is correspondingly explained as a change in the population of these conformational substates.[2]

For comparison to human hemoglobin we examined cryoreduced bovine, pigeon, and carp HbO_2. The mammalian and avian HbO_2 behave like the human protein, but the piscine HbO_2 shows only an A-like EPR signal (Table S1), and this is unchanged in the presence of glycols.

Isolated αO_2 and βO_2 Chains and MbO_2. The idea that the oxyheme centers of *each* subunit exhibit two major conformational substates is confirmed by the observation of A- and B-type signals upon cryoreduction of highly purified isolated chains (Figure 2) and of diliganded, mixed-metal/valency hybrids (Figure 3). Cryoreduced βO_2 chains in frozen buffer solution exhibit majority A-like and minority B-like

[2] It should be also noted that EPR spectra of cryoreduced HbO_2 were independent of the protein concentration in the range of 0.5−6 mM. This finding rules out the possible effect of the tetramer−dimer equilibrium.

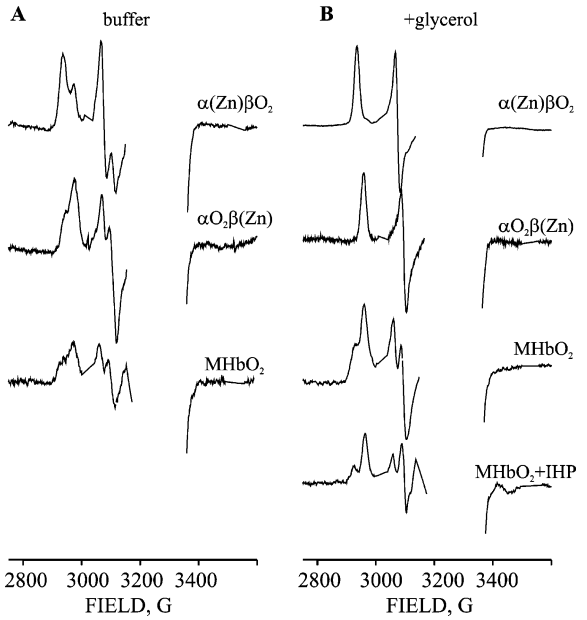

FIGURE 3: X-band EPR spectra of cryoreduced $\alpha O_2\beta$(Zn), α-(Zn)βO_2 hybrids and Milwaukee HbO_2 ($MHbO_2$) in frozen buffer (50 mM BisTris, pH 7) (panel A) and in the presence 16% glycerol (panel B). Instrument settings as in Figure 1.

EPR signals, and the reverse is true for αO_2 chains (Figure 2A).[3] The *g*-values of the A and B substate signals in the cryoreduced αO_2 chains differ slightly but reproducibly from those in the EPR spectra of cryoreduced βO_2 chains and HbO_2 (Table S1), indicating that the A and B conformational substates in αO_2 and βO_2 chains, though similar, are not structurally identical.

The spectrum of HbO_2 in buffer (Figure 1) can be well reproduced by adding equal amounts of the spectra of αO_2 and βO_2 chains, as expected if the two chains have the same reduction efficiency. Conversely, subtraction of the βO_2 signal from that of HbO_2 gives a spectrum whose A and B components have very similar *g*-values to those for cryoreduced isolated αO_2 chains. As the *g*-values of the A- and B-type EPR signals of the αO_2 chains in buffer are slightly but reproducibly different from those for the A signals in the EPR spectra of cryoreduced βO_2 chains (Table S1), these observations confirm the presence of a minority αO_2^A substate *within* αO_2 *chains of the* HbO_2 *tetramer*.

Glycerol and ethylene glycol additives enhance the relative population of the A-type substate for both chains (Figure 2B) but much more so for β chains; for βO_2, the signal becomes almost pure A type, whereas for αO_2, the intensities equalize. The spectrum for HbO_2 in glycerol (Figure 1A) is qualitatively reproduced by summing the spectra of the chains in glycerol, indicating that assembly of chains into the R-structure does not introduce a quaternary influence on the substate populations of the oxyheme centers. As expected, IHP has no influence on the spectra of isolated chains.

We corroborated the previous observation (*2*) that the EPR signal of cryoreduced oxymyoglobin displays a B-like EPR signal, with $g = [1.969, 2.118, 2.218]$, but also a minority A-like component (Table S1) and that the population of the minority species depends slightly on pH and glycol additives (not shown).

Mixed-Metal and Valency Hybrids of HbO_2. Possible quaternary influences/constraints on substate populations have been probed by studies of T-structure Hb hybrids. Figure 3 shows EPR spectra for cryoreduced [αO_2,β(Zn)] and [α(Zn),βO_2] hybrids. Whereas isolated αO_2 and βO_2 chains resemble the chains in fully liganded HbO_2, which has the R-structure (*32*−*34*), these diliganded hybrids adopt the T quaternary structure (*35*, *36*). In addition, there are spectra for M-Milwaukee HbO_2, [αO_2,$\beta^{67Val-Glu}(Fe^{3+})$] (M HbO_2), which also has a T-like structure (*22*, *37*).

The EPR spectra of these cryoreduced T-structure hybrids in frozen buffer exhibit both A- and B-like signals, with relative intensities that are similar to those of the corresponding isolated chains (Figure 2). Moreover, a 1/1 sum of the spectra for the α-O_2 and β-O_2 T-hybrids would roughly match the A/B $\sim$ 1/1 ratio for R-structure HbO_2 in frozen buffer, again as expected if the oxyheme units in both subunits are cryoreduced with the same efficiency. Thus for hemoglobin in buffer solution, the formation of the tetramer and its conversion between R and T quaternary structures do not appear to influence the oxyheme substate populations. In addition, the minimal variation in *g*-values (Table S1) indicates that the electronic properties of the individual substates are largely, although not completely, independent of the quaternary structure.

Glycols as cosolvents, however, do influence substate populations. In the presence of 16% glycerol, the diliganded T-structure [α(Zn),βO_2] hybrid adopts only the A substate, just like the R-like isolated βO_2 chains; in glycerol buffer, the αO_2 subunits of the T-structure [αO_2,β(Zn)] hybrid completely convert to the B substate, whereas the isolated αO_2 chains still show both substates. The *g*-values of the αO_2^B substate also differ somewhat from these for the B substates in isolated αO_2 chains and the HbO_2 tetramer (Table S1). Thus, the presence of glycerol causes a similar alteration in the βO_2 heme pocket of isolated chains and of the hybrid, but the αO_2 heme pocket of the T-structure hybrid undergoes a greater change in substate populations than that of isolated chains. It appears, therefore, that formation of the T-structure tetramer does not alter the substate ratio for α chains but it does "sensitize" these chains to the perturbing influence of glycols.

The EPR spectrum of the cryoreduced [αO_2,$\beta^{67Val-Glu}(Fe^{3+})$] hybrid in frozen buffer at pH 7 is like that of the [αO_2,β-(Zn)] hybrid in having a B-like majority substate (Figure 3A), and likewise, addition of glycerol results in an increase in the B-type EPR contribution, but not to 100%. Addition of IHP to the Hb-M hybrid, which stabilizes the T-structures, results in further increase in the relative populations of αO_2^B species (Figure 3B) and causes changes in the *g*-tensor components of the B-species (Table S1).

^{1}H ENDOR. To characterize distal pocket H-bonding to the HbO_2 oxyferroheme, we have employed 35 GHz ^{1}H ENDOR spectroscopy to examine the peroxoferriheme primary cryoreduction products. Figure 4 shows ^{1}H ENDOR spectra collected at numerous fields across the EPR envelope of the cryoreduced β chains in 16% glycerol/buffer mixture, which exhibit only an A EPR signal. The g_1 spectrum shows a poorly resolved ^{1}H ENDOR signal centered at ν_H with a spread of $A \lesssim 5$ MHz, plus a strongly coupled $\nu_\pm$ proton

[3] The relative population of the minority A species for oxy-β chains increases as the pH is raised from 6 to 8 (not shown).

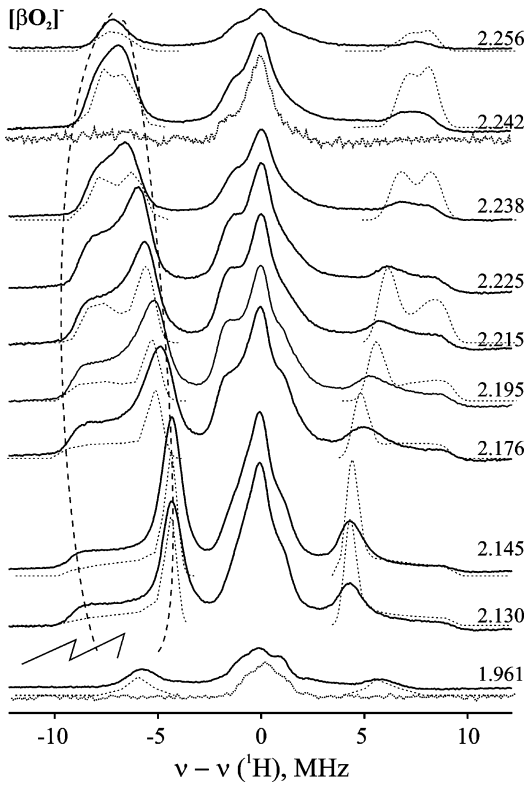

FIGURE 4: Orientation-selective, 2D field/frequency ^{1}H CW ENDOR patterns for cryoreduced βO_2 chains in 16% glycerol/H_2O buffer (solid line) and glycerol-d_3/D_2O buffer (dotted line). These experiments exclude fields between roughly g_2 and g_3 because of strong EPR signals from free radicals generated by the irradiation that occurs in this range. Instrument settings: 35.21 GHz, 2 K, 100 kHz field modulation, 1.5 G modulation amplitude, 1 MHz/s scan speed, 30 db microwave power, 10 W RF power, 200 kHz broadening of RF excitation, and 10 scans. Simulated spectra (see text) are shown by dashed lines.

doublet split by hyperfine coupling of $A(g_1) \approx 14$ MHz. As illustrated by spectra shown for the sample prepared in ^2H_2O buffer, the proton signals with $A < 5$ MHz include intensity from both exchangeable and nonexchangeable protons, whereas the proton signals with $A > 5$ MHz are completely exchangeable. The strongly coupled proton is assigned to the distal histidine N$^\epsilon$H hydrogen-bonded to the O_2 ligand in the parent (*2*, *16*). The $\nu_\pm$ peaks at ± 7 MHz seen at g_1 ($A \approx 14.5$ MHz) for the H-bond proton split into two branches as g decreases. Focusing on the ν_- feature, as g is decreased toward the vicinity of g_2, the outer branch smoothly moves to a minimum frequency, corresponding to the maximum component of the hyperfine tensor, $A = 19$ MHz, whereas the inner branch increases in frequency (decreasing A). Spectra taken near g_3 again show a single $\nu_\pm$ doublet, $A(g_3) = 13.4$ MHz. Numerous simulations of the field-dependent pattern lead to a best fit which employed a nearly axial hyperfine tensor (Table 2) with $a_{iso} = 11.8$ MHz. As can be seen in Figure S1 (Supporting Information), this tensor gives a remarkably good representation of the experiments.

Figure 5 shows that the corresponding 2D ^{1}H ENDOR pattern for the cryoreduced, B-substate, [αO_2,β(Zn)] hybrid (16% glycerol/buffer mixture) is quite distinct from those for the A-type centers. Simulation of the B pattern led to a best fit with the hyperfine tensor, given in Table 3, with a 2-fold smaller isotropic coupling, $a_{iso} = 5.8$ MHz (Figure S2). A qualitatively similar 2D ^{1}H ENDOR pattern is shown by the dominant B substate of cryoreduced MbO_2 (Figure S3, Supporting Information; Table 3),with $a_{iso} = 2.9$.

Table 2: ^{1}H Hyperfine Interaction Parameters for the Exchangeable H-Bond Proton

protein	a_{iso} (MHz)	A_1	A_2	A_3	θ (deg)	ϕ (deg)[a]
A-type						
βO_2[b]	11.8	8.2	8.5	18.8	37	0
B-type						
$\alpha O_2\beta$(Zn)	5.8	1	3	13.4	80	0
MbO_2	2.9	−1.5	−1.5	11.6	83	0

[a] The polar angle, θ, is measured relative to the g_1 direction, which lies roughly along the heme normal; the angle ϕ is defined as a rotation about g_1. [b] Identical results were obtained for isolated βO_2 chains (βO_2 tetramer) and for the α(Zn)βO_2 hybrid.

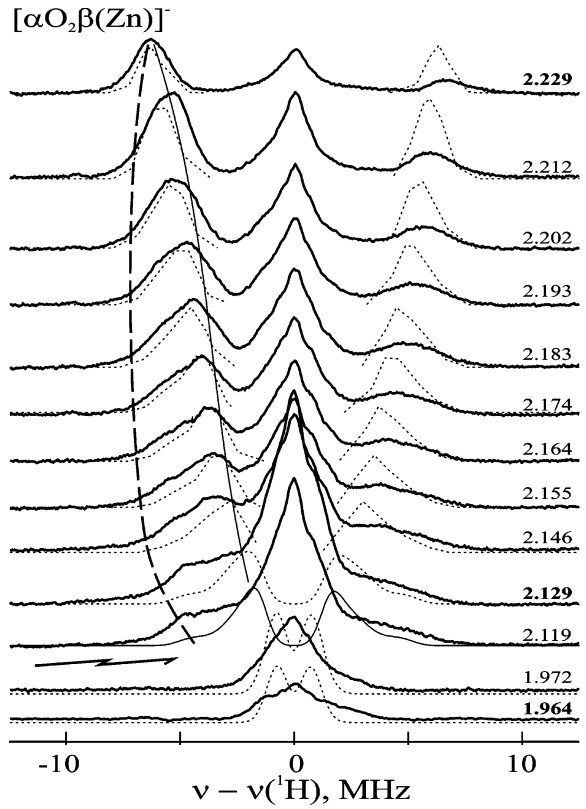

FIGURE 5: Orientation-selective, 2D field/frequency ^{1}H CW ENDOR patterns for the cryoreduced $\alpha O_2\beta$(Zn) hybrid in 16% glycerol/buffer (pH 7). Instrument settings as in Figure 4.

The ca. 2-fold difference in isotropic couplings for the A- and B-type centers, $a^A_{iso} \approx 12$ MHz and $a^B_{iso} \approx 3-6$ MHz, and notably different tensor orientations (values of θ) likely are a consequence of different geometries of the hydrogen bond between the distal histidine and O−O moiety. The characteristic ^{1}H ENDOR spectra of A-type centers can be easily recognized in ENDOR spectra of samples that contain both A- and B-like centers, as seen in the $g = 2.206$ ^{1}H ENDOR spectra for several A-centers (Figure 6). All of these proteins, whose αO_2 subunits reveal a minority αO_2^A population, show a strongly coupled proton signal similar to the βO_2^A center overlaid on the ENDOR response from the majority αO_2^B center. This observation gives evidence of structural similarity of the hydrogen bonds between the N−H of the distal histidine proton and peroxo moieties in the minority αO_2^A and majority βO_2^A substates.

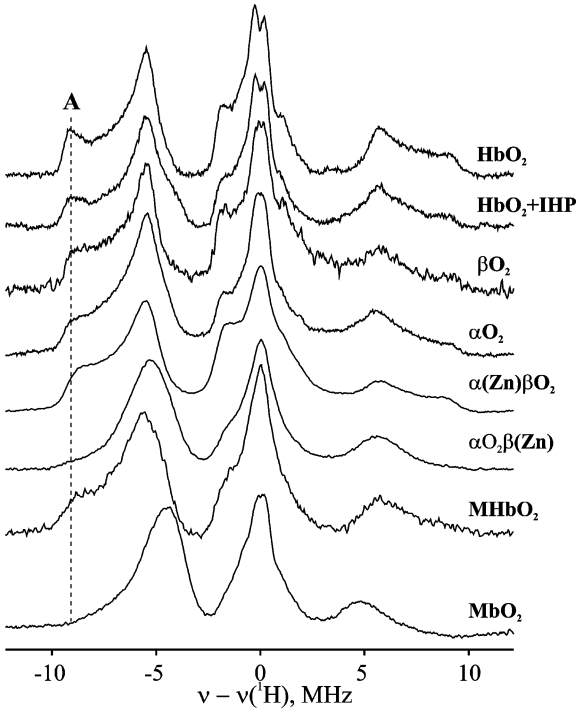

FIGURE 6: ^{1}H CW ENDOR spectra of selected cryoreduced oxyhemoproteins taken at $g = 2.206$. Conditions: 0.05 M BisTris, pH 7, and 16% glycerol. Instrument settings as in Figure 4.

DISCUSSION

Cryoreduction of a diamagnetic oxyheme center in HbO_2 and its chains produces an unrelaxed EPR-active peroxoferriheme center that retains the main structural characteristics of the oxyferroheme parent. The present results establish that the hemoglobin αO_2 and βO_2 subunit oxyferroheme *both* adopt two major conformational substates, denoted A and B: upon cryoreduction, the A-substate oxyheme centers, αO_2^A and βO_2^A, show similar although not identical rhombic EPR signals, and the same is true for αO_2^B and βO_2^B substates. The average *g*-values for the A/B classes of peroxoferrihemes are listed in Table 1.

In frozen buffer the B substate is dominant in αO_2 subunits/chains, while A dominates in βO_2. A simple ligand-field analysis (*38*) discloses that these different *g*-tensors do not correspond to different ligand fields (within error) but rather to slightly differing covalency parameters. This suggests that they reflect slightly different orientations, and hence bonding, to the peroxo moiety. The associated differences in H-bonding between the O−O moiety and the distal histidine are distinctly seen in the ^{1}H ENDOR characterization of the H-bond proton (Table 2).

Our determination that both types of isolated chains exhibit the two oxyheme substates corrects previous conclusions. In the case of isolated βO_2 chains, it is likely that the previous experiments failed to observe the minor B-like EPR signals (*1*, *2*) because the samples were chiefly prepared with ethylene glycol/buffer mixtures, which suppress the B-like signal. The only report, to our knowledge, of results on isolated αO_2 chains (*1*) did not give enough details to suggest reasons why the two substates were not observed.

Addition of glycols does not perturb the oxyheme centers, as shown by the constancy of the *g*-tensors. However, glycerol and especially ethylene glycol induce dramatic changes in the relative populations of the A- and B-like oxyheme centers, an effect that is observed at relatively low concentrations of these additives [2.5% (v/v)]. Further, addition of the sugars glucose, sucrose and trehalose causes negligible change in the relative populations of the conformational substates of oxyHb in frozen buffer. The addition of IHP to oxy-Hb solutions largely suppresses the influence of glycol cosolvents, while curiously enabling some influences of the sugars.

The glycols/sugars were shown to be osmolytes, solutes soluble only in bulk water, not in the protein hydration layer (*39*, *40*). Such compounds decrease the affinity of deoxyhemoglobin for O_2, and it has been suggested that they do so through a reduction of the water activity rather than direct solute interaction with the protein (*40*−*43*). The stronger effect of ethylene glycol and glycerol on cryoreduced HbO_2, relative to sugars, suggests that the mode of action of these cosolvents is not restricted to changes of water activity but may be due to the specific interactions with the macromolecule. X-ray diffraction data for some proteins crystallized in water/glycerol solution disclose that one or several molecules of the cosolvent may associate more or less specifically to surface residues (*44*−*46*). Similarly, the alcohols were shown to stabilize oxyhemoglobin against autoxidation (*47*, *48*). In the case of metHb an addition of glycerol causes changes of both the tertiary and secondary (α-helix) conformations of the protein and increases its gyration radius (*49*).

In the presence of glycols, isolated β chains (β_4 tetramers) and T-structure [α(Zn),βO_2] hybrids both show only the A substate. In contrast, isolated αO_2 chains show roughly 1/1, A/B populations when glycerol is present, while the T-structure mixed-metal [αO_2,βZn] hybrid and valency hybrid, Hb M-Milwaukee (*22*, *37*), show only the B substate in the presence of glycerol. The glycols also slightly modulate the *g*-tensor of the cryoreduced αO_2^B center (Table S1). Taken together, these results suggest a quaternary influence on the oxyheme distal pocket of α chains and that the glycol-induced changes in the substate populations of the R-state HbO_2 tetramer are largely associated with the αO_2 subunit. This conclusion correlates with numerous observations on HbNO and $CoHbO_2$ which demonstrate that the α subunit has a more flexible conformation than the β subunit (*50*−*54*). In this context, it is worth noting that although the spread around the average *g*-values for each substate is not large, the *g*-tensor components for A-type (as well as B-type) oxyheme centers in the α and β subunits are similar but not identical, indicating that the conformational substates αO_2^A and βO_2^A (αO_2^B and βO_2^B) differ in structure as well as in affinity for O_2.

The ^{1}H ENDOR data indicate that the H-bonding to dioxygen is essentially the same in all A-substate oxyheme centers, whether in αO_2 or βO_2, and that the same is probably true for the B-substate centers. However, the interactions between the distal histidine and the O_2 ligand are quite different in an A and a B substate. This is consistent with other observations, including crystal structure data, about differences in the hydrogen bonds in the α and β subunits, the former being majority B substate and the latter A substate (*55*−*58*). The large values of a_{iso} for both A and B conformers are well-known and reflect spin delocalization onto the [O−O] moiety (*13*, *14*). The larger isotropic coupling in the A-type center likely reflects a combination of two factors:

(i) the H-bond is directed more toward the proximal, spin-bearing O atom; (ii) the H-bonded proton lies farther from the Fe−O−O plane and thus out of the nodal plane of the spin-bearing π orbital on the proximal O.

The demonstration of conformational variability of oxyheme centers in human oxy-Hb and its chains extends the longstanding recognition of such phenomenon for hemes with CO bound as the distal ligand (*17*, *18*, *59*−*62*). IR spectra of carboxy-Mb and Hb disclosed several conformational substates with different ν_{C-O} peaks (*17*, *18*, *63*). The calculations carried out by Oldfield (*18*), Olson (*19*, *64*), Sigfridsson (*65*), and Stavrov (*66*) have shown that conformational substates are associated with the multiple orientations and tautomeric forms of the distal histidine which create a different electrostatic field around the bound CO. Analysis of the high-resolution (better than 1.2 Å) crystallographic data on MbCO and MbO_2 shows discrete disorder of the distal histidine, revealing several distinct conformers of the imidazole side chain (*67*, *68*). Likewise, it has long been known that NO does not adopt a single conformation when bound to heme (*69*, *70*).

An indirect, kinetic, but *not* spectroscopic, indication of conformational variability has been reported for MbO_2 (*71*) as has the observation of two different orientations for bound dioxygen in oxy-[Fe(TpivPP)(2-MeIM)] (*72*−*75*). Presumably, the low resolution of the available crystal structures for HbO_2 has prevented the resolution of the individual substates of the oxyheme centers and their distal and proximal environments. In addition, DFT calculations show stronger electrostatic interaction between the distal histidine and the bound O_2 due to polarization of the Fe−O bond (*65*, *76*). This may sharpen energy minima for bound O_2 and explain why bound O_2 has a smaller number of major substates (2) than does bound CO (>3).

ACKNOWLEDGMENT

We acknowledge Prof. H. Halpern (University of Chicago) for access to a Gammacell 220 ^{60}Co irradiator.

SUPPORTING INFORMATION AVAILABLE

One table listing *g*-tensor components for primary cryoreduced oxyheme centers in oxyhemoglobin and related compounds and three figures showing orientation-selective, 2D field/frequency ^{1}H CW ENDOR patterns for cryoreduced isolated βO_2 chains, the $\alpha O_2\beta$(Zn) hybrid, and MbO_2. This material is available free of charge via the Internet at http://pubs.acs.org.

REFERENCES

1. Symons, M. C. R., and Petersen, R. L. (1978) Electron capture by Oxyhaemoglobin: an e.s.r. study, *Proc. R. Soc. London, Ser. B 201*, 285−300.
2. Kappl, R., Höhn-Berlage, M., Hüttermann, J., Bartlett, N., and Symons, M. C. R. (1985) Electron spin and electron nuclear-double resonance of the $[FeO_2]^-$ centre from irradiated oxyhemo- and oxymyoglobin, *Biochim. Biophys. Acta 827*, 327−343.
3. Davydov, R. M. (1980) Optical and EPR Spectroscopy of the Electron Adducts of Oxymyoglobin and Oxy Haemoglobin, *Biofizika 25*, 203−207.
4. Davydov, R., Kappl, R., Hutterman, R., and Peterson, J. (1991) EPR spectroscopy of reduced oxyferrous cytochrome P 450cam, *FEBS Lett. 295*, 113−115.
5. Davydov, R., Makris, T. M., Kofman, V., Werst, D. W., Sligar, S. G., and Hoffman, B. M. (2001) Hydroxylation of Camphor by Reduced oxy-Cytochrome P450cam: Mechanistic Implications of EPR and ENDOR of Catalytic Intermediates in Native and Mutant Enzymes, *J. Am. Chem. Soc. 123*, 1403−1415.
6. Davydov, R., Kofman, V., Fujii, H., Yoshida, T., Ikeda-Saito, M., and Hoffman, B. M. (2002) Catalytic Mechanism of Heme Oxygenase through EPR and ENDOR of Cryoreduced Oxy-Heme Oxygenase and its Asp140 Mutants, *J. Am. Chem. Soc. 124*, 1798−1808.
7. Davydov, R., Ledbetter-Rogers, A., Martasek, P., Larukhin, M., Sono, M., Dawson, J. H., Masters, B. S. S., and Hoffman, B. M. (2002) EPR and ENDOR Characterization of Intermediates in the Cryoreduced Oxy-Nitric Oxide Synthase Heme Domain with Bound L-Arginine or NG-Hydroxyarginine, *Biochemistry 41*, 10375−10381.
8. Symons, M. C. R., and Petersen, R. L. (1978) Electron capture at the iron−oxygen center in single crystals of oxymyoglobin studied by electron spin resonance spectroscopy, *Biochim. Biophys. Acta 535*, 241−246.
9. Bartlett, N., and Symons, M. C. R. (1983) Electron addition to the (FeO2) unit of oxyhemoglobin Glycera, *Biochim. Biophys. Acta 744*, 110−114.
10. Symons, M. C. R., and Petersen, R. L. (1978) The relative electron affinities of the α and β chains of oxyhemoglobin as a function of pH and added inositol hexaphosphate. An electron spin resonance study, *Biochim. Biophys. Acta 537*, 70−76.
11. Bartlett, N., Stephenson, J. M., and Symons, M. C. R. (1989) Effect of ionizing radiation on hemoglobin: the oxy-derivative of hemoglobin Iwate, *Proc. R. Soc. London, Ser. B: Biol. Sci. 238*, 103−112.
12. Gasyna, Z. (1979) Intermediate spin-states in one-electron reduction of oxygen-hemoprotein complexes at low temperature, *FEBS Lett. 106*, 213−218.
13. Leibl, W., Nitschke, W., and Hüttermann, J. (1986) Spin-density distribution in the $[FeO_2]^-$ complex. Electron spin resonance of myoglobin single crystals, *Biochim. Biophys. Acta 870*, 20−30.
14. Davydov, R., Satterlee, J. D., Fujii, H., Sauer-Masarwa, A., Busch, D. H., and Hoffman, B. M. (2003) A Superoxo-Ferrous State in a Reduced Oxy-Ferrous Hemoprotein and Model Compounds, *J. Am. Chem. Soc. 125*, 16340−16346.
15. Norris, L., Davydov, R., and Hoffman, B. M. (2004) manuscripts in preparation.
16. Davydov, R. M., Yoshida, T., Ikeda-Saito, M., and Hoffman, B. M. (1999) Hydroperoxy-Heme Oxygenase Generated by Cryoreduction Catalyzes the Formation of α-meso-Hydroxyheme as Detected by EPR and ENDOR, *J. Am. Chem. Soc. 121*, 10656−10657.
17. Ansari, A., Berendzen, J., Braunstein, D., Cowen, B. R., Frauenfelder, J., Hong, M. K., Iben, I. E. T., Johnson, J. B., Ormos, P., Sauke, T. B., Scholl, R., Schulte, A., Steinbach, P. J., Vittitow, J., and Yound, R. D. (1987) Rebinding and Relaxation in the Myoglobin Pocket, *Biophys. Chem. 26*, 337−355.
18. Oldfield, E., Guo, K., Augspurger, J. D., and Dykstra, C. E. (1991) A molecular model for the major conformational substates in heme proteins, *J. Am. Chem. Soc. 113*, 7537−7541.
19. Phillips, G. N., Jr., Teodoro, M. L., Li, T., Smith, B., and Olson, J. S. (1999) Bound CO Is A Molecular Probe of Electrostatic Potential in the Distal Pocket of Myoglobin, *J. Phys. Chem. B 103*, 8817−8829.
20. Doyle, M. L., Lew, G., Deyoung, A., Kwiatkowski, L., Wierzba, A., Noble, R. W., and Ackers, G. K. (1992) Functional Properties of Human Hemoglobins Synthesized From Recombinant Mutant Beta-Globins, *Biochemistry 31*, 8629−8639.
21. Noble, R. W., Hui, H. L., Kwiatkowski, L. D., Paily, P., DeYoung, A., Wierzba, A., Colby, J. E., Bruno, S., and Mozzarelli, A. (2001) Mutational Effects at the Subunit Interfaces of Human Hemoglobin: Evidence for a Unique Sensitivity of the T Quaternary State to Changes in the Hinge Region of the $\alpha 1\beta 2$ Interface, *Biochemistry 40*, 12357−12368.
22. John, M. E., and Waterman, M. R. (1980) Structural basis for the conformational states of nitrosyl hemoglobins M Saskatoon and M Milwaukee. Influence of distal histidine residues on proximal histidine-iron bonds, *J. Biol. Chem. 255*, 4501−4506.
23. Noble, R. W., De Young, A., Vitale, S., Morante, S., and Cerdonio, M. (1987) Studies on the linkage between spin equilibria and protein structure in carp ferric hemoglobin, *Eur. J. Biochem. 168*, 563−567.
24. Davydov, R., Valentine, A. M., Komar-Panicucci, S., Hoffman, B. M., and Lippard, S. J. (1999) An EPR Study of the Dinuclear Iron Site in the Soluble Methane Monooxygenase from *Methy-*

lococcus capsulatus (Bath) Reduced by One Electron at 77K: The Effects of Component Interactions and the Binding of Small Molecules to the Diiron(III) Center, *Biochemistry 38*, 4188−4197.
25. Werst, M. M., Davoust, C. E., and Hoffman, B. M. (1991) Ligand Spin Densities in Blue Copper Proteins by Q-band ^{1}H and ^{14}N ENDOR Spectroscopy, *J. Am. Chem. Soc. 113*, 1533−1538.
26. Hoffman, B. M., DeRose, V. J., Ong, J. L., and Davoust, C. E. (1994) Sensitivity Enhancement in Field-Modulated CW ENDOR via RF Bandwidth Broadening, *J. Magn. Reson. 110*, 52−57.
27. Abragam, A., and Bleaney, B. (1970) *Electron Paramagnetic Resonance of Transition Metal Ions*, 2nd ed., Clarendon Press, Oxford.
28. Hoffman, B. M., Gurbiel, R. J., Werst, M. M., and Sivaraja, M. (1989) in *Advanced EPR. Applications in Biology and Biochemistry* (Hoff, A. J., Ed.) pp 541−591, Elsevier, Amsterdam.
29. Hoffman, B. M. (1991) Electron nuclear double resonance (ENDOR) of metalloenzymes, *Acc. Chem. Res. 24*, 164−170.
30. Hoffman, B. M., DeRose, V. J., Doan, P. E., Gurbiel, R. J., Houseman, A. L. P., and Telser, J. (1993) Metalloenzyme Active-Site Structure and Function through Multifrequency CW and Pulsed ENDOR, *Biol. Magn. Reson. 13*, 151−218.
31. Davydov, R., Kuprin, S., Graslund, A., and Ehrenberg, A. (1994) EPR study of the mixed-valent diiron center in E. coli RNR produced by reduction of radical-free protein R2 at 77 K., *J. Am. Chem. Soc. 116*, 11120−1128.
32. Valdes, R., Jr., and Ackers, G. K. (1977) Thermodynamic studies on subunit assembly in human hemoglobin. Self-association of oxygenated chains (αSH and βSH): determination of stoichiometries and equilibrium constants as a function of temperature, *J. Biol. Chem. 252*, 74−81.
33. Antonini, E., and Brunori, M. (1971) *Hemoglobin and Myoglobin in Their Reactions with Ligands*, North-Holland Publishing Co., Amsterdam.
34. Borgstahl, G. E. O., Rogers, P. H., and Arnone, A. (1994) The 1.8 Å structure of carbonmonoxy-β_4 hemoglobin. Analysis of a homotetramer with the R quaternary structure of liganded $\alpha_2\beta_2$ hemoglobin, *J. Mol. Biol. 236*, 817−830.
35. Arnone, A., Rogers, P., Blough, N. V., McGourty, J. L., and Hoffman, B. M. (1986) X-ray Diffraction Studies of a Partially Liganded Hemoglobin, $[\alpha(\text{FeII-CO})\beta(\text{MnII})]_2$, *J. Mol. Biol. 188*, 693−706.
36. Miyazaki, G., Morimoto, H., Yun, K.-M., Park, S.-Y., Nakagawa, A., Minagawa, H., and Shibayama, N. (1999) Magnesium(II) and Zinc(II)-Protoporphyrin IX's Stabilize the Lowest Oxygen Affinity State of Human Hemoglobin Even More Strongly than Deoxyheme, *J. Mol. Biol. 292*, 1121−1136.
37. Perutz, M. F., Pulsinelli, P. D., and Ranney, H. M. (1972) Structure and subunit interaction of hemoglobin M Milwaukee, *Nat. New Biol. 237*, 259−263.
38. McGarvey, B. R. (1998) Survey of ligand field parameters of strong field d^5 complexes obtained from the *g* matrix, *Coord. Chem. Rev. 170*, 75−92.
39. Timasheff, S. N. (2002) Protein Hydration, Thermodynamic Binding, and Preferential Hydration, *Biochemistry 41*, 13473−13482.
40. Parsegian, V. A., Rand, R. P., and Rau, D. C. (1995) Macromolecules and water: probing with osmotic stress, *Methods Enzymol. 259*, 43−94.
41. Colombo, M. F., Rau, D. C., and Parsegian, V. A. (1992) Protein solvation in allosteric regulation: a water effect on hemoglobin, *Science 256*, 655−659.
42. Colombo, M. F., and Seixas, F. A. V. (1999) Novel allosteric conformation of human Hb revealed by the hydration and anion effects on O_2 binding, *Biochemistry 38*, 11741−11748.
43. Biswal, B. K., and Vijayan, M. (2002) Structures of human oxy- and deoxyhemoglobin at different levels of humidity: variability in the T state, *Acta Crystallogr., Sect. D: Biol. Crystallogr. 58*, 1155−1161.
44. Charron, C., Kadri, A., Robert, M. C., Giege, R., and Lorber, B. (2002) Crystallization in the presence of glycerol displaces water molecules in the structure of thaumatin, *Acta Crystallogr., Sect. D: Biol. Crystallogr. 58*, 2060−2065.
45. Adler, M., Davey, D. D., Phillips, G. B., Kim, S.-H., Jancarik, J., Rumennik, G., Light, D. R., and Whitlow, M. (2000) Preparation, Characterization, and the Crystal Structure of the Inhibitor ZK-807834 (CI-1031) Complexed with Factor Xa, *Biochemistry 39*, 12534−12542.
46. Vidakovic, M., Sligar, S. G., Li, H., and Poulos, T. L. (1998) Understanding the Role of the Essential Asp251 in Cytochrome P450cam Using Site-Directed Mutagenesis, Crystallography, and Kinetic Solvent Isotope Effect, *Biochemistry 37*, 9211−9219.
47. Nedjar-Arroume, N., Castellano, A., and Guillochon, D. (1995) Stabilizing effect of water/alcohol solvents towards autoxidation of glutaraldehyde-modified hemoglobin, *Biotechnol. Appl. Biochem. 21*, 173−183.
48. Nedjar-Arroume, N., Castellano, A., Piot, J. M., and Guillochon, D. (1993) Stabilizing effect of water/alcohol solvents towards autoxidation of human hemoglobin, *Biotechnol. Appl. Biochem. 18*, 25−35.
49. Barteri, M., Gaudiano, M. C., and Santucci, R. (1996) Influence of glycerol on the structure and stability of ferric horse heart myoglobin: a SAXS and circular dichroism study, *Biochim. Biophys. Acta 1295*, 51−58.
50. Kappl, R., and Hütterman, J. (1989) in *Advanced EPR: Applications in Biology and Biochemistry* (Hoff, A. J., Ed.) pp 501−540, Elsevier, Amsterdam.
51. Yonetani, T., Tsuneshige, A., Zhou, Y., and Chen, X. (1998) Electron Paramagnetic Resonance and Oxygen Binding Studies of α-Nitrosyl Hemoglobin, *J. Biol. Chem. 273*, 20323−20333.
52. Henry, Y., and Banerjee, R. (1973) Electron paramagnetic studies of nitric oxide hemoglobin derivatives. Isolated subunits and nitric oxide hybrids, *J. Mol. Biol. 73*, 469−82.
53. De Sanctis, G., Priori, A. M., Polizio, F., Ascenzi, P., and Coletta, M. (1998) Different structural effects of allosteric modulators on subunits of tetrameric ferrous nitrosylated human hemoglobin: an EPR spectroscopic study, *J. Biol. Inorg. Chem. 3*, 135−139.
54. Cassoly, R. (1975) Relations between optical spectrum and structure in nitrosyl hemoglobin and hybrids, *J. Mol. Biol. 98*, 581−595.
55. Shaanan, B. (1983) Structure of human oxyhemoglobin at 2.1 Å resolution, *J. Mol. Biol. 171*, 31−59.
56. Perutz, M. F., Fermi, G., Luisi, B., Shaanan, B., and Liddington, R. C. (1987) Stereochemistry of Cooperative Mechanisms in Hemoglobin, *Acc. Chem. Res. 20*, 309−321.
57. Lukin, J. A., Simplaceanu, V., Zou, M., Ho, N. T., and Ho, C. (2000) NMR reveals hydrogen bonds between oxygen and distal histidines in oxyhemoglobin, *Proc. Natl. Acad. Sci. U.S.A. 97*, 10354−10358.
58. Paoli, M., Liddington, R., Tame, J., Wilkinson, A., and Dodson, G. (1996) Crystal structure of T state hemoglobin with oxygen bound at all four hemes, *J. Mol. Biol. 256*, 775−792.
59. Shimizu, H., Park, S. Y., Shiro, Y., and Adachi, S. i. (2002) X-ray structure of nitric oxide reductase (cytochrome P450nor) at atomic resolution, *Acta Crystallogr., Sect. D: Biol. Crystallogr. 58*, 81−89.
60. Godbout, N., Sanders, L. K., Salzmann, R., Havlin, R. H., Wojdelski, M., and Oldfield, E. (1999) Solid-State NMR, Mossbauer, Crystallographic, and Density Functional Theory Investigation of Fe-O_2 and Fe-O_2 Analog Metalloporphyrins and Metalloproteins, *J. Am. Chem. Soc. 121*, 3829−3844.
61. Miller, L. M., Pedraza, A. J., and Chance, M. R. (1997) Identification of Conformational Substates Involved in Nitric Oxide Binding to Ferric and Ferrous Myoglobin through Difference Fourier Transform Infrared Spectroscopy (FTIR), *Biochemistry 36*, 12199−12207.
62. Couture, M., Burmester, T., Hankeln, T., and Rousseau, D. L. (2001) The heme environment of mouse neuroglobin. Evidence for the presence of two conformations of the heme pocket, *J. Biol. Chem. 276*, 36377−36382.
63. Zentz, C., El Antri, S., Pin, S., Cortes, R., Massat, A., Simon, M., and Alpert, B. (1991) Alteration of heme axial ligands in hemoglobin by organic solvents analyzed by CD, FTIR and XANES techniques, *Biochemistry 30*, 2804−2810.
64. Olson, J. S., and Phillips, G. N. J. (1997) Myoglobin discriminates between O_2, NO and CO by electrostatic interactions with the bound ligand, *J. Biol. Inorg. Chem. 2*, 544−552.
65. Sigfridsson, E., and Ryde, U. (1999) On the significance of hydrogen bonds for the discrimination between CO and O_2 by myoglobin, *J. Biol. Inorg. Chem. 4*, 99−110.
66. Kushkuley, B., and Stavrov, S. S. (1996) Theoretical study of the distal-side steric and electrostatic effects on the vibrational characteristics of the FeCO unit of the carbonylheme proteins and their models, *Biophys. J. 70*, 1214−1229.
67. Vojtechovsky, J., Chu, K., Berendzen, J., Sweet, R. M., and Schlichting, I. (1999) Crystal structures of myoglobin-ligand complexes at near-atomic resolution, *Biophys. J. 77*, 2153−2174.

68. Kachalova, G. S., Popov, A. N., and Bartunik, H. D. (1999) A steric mechanism for inhibition of CO binding to heme proteins, *Science 284*, 473−476.
69. Hori, H., Ikeda-Saito, M., and Yonetani, T. (1981) Electromagnetic properties of hemoproteins. VI. Single-crystal EPR of myoglobin nitroxide. Freezing-induced reversible changes in the molecular orientation of the ligand, *J. Biol. Chem. 256*, 7849−7855.
70. Huttermann, J., Burgard, C., and Kappl, R. (1994) Proton ENDOR from randomly oriented NO-ligated hemoglobin: approaching the structural basis for the R-T transition, *J. Chem. Soc., Faraday Trans. 90*, 3077−3087.
71. Miller, L. M., Patel, M., and Chance, M. R. (1996) Identification of Conformational Substates in Oxymyoglobin through the pH-Dependence of the Low-Temperature Photoproduct Yield, *J. Am. Chem. Soc. 118*, 4511−4517.
72. Collman, J. P., Gagne, R. R., Reed, C. A., Robinson, W. T., and Rodley, G. A. (1974) Structure of an iron(II) dioxygen complex. Model for oxygen carrying hemeproteins, *Proc. Natl. Acad. Sci. U.S.A. 71*, 1326−1329.
73. Jameson, G. B., Rodley, G. A., Robinson, W. T., Gagne, R. R., Reed, C. A., and Collman, J. P. (1978) Structure of a dioxygen adduct of (1-methylimidazole)-meso-tetrakis(α,α,α,α-o-pival-amidophenyl)porphinatoiron(II). An iron dioxygen model for the heme component of oxymyoglobin, *Inorg. Chem. 17*, 850−857.
74. Spartalian, K., Lang, G., Collman, J. P., Gagne, R. R., and Reed, C. A. (1975) Moessbauer spectroscopy of hemoglobin model compounds. Evidence for conformational excitation, *J. Chem. Phys. 63*, 5375−5382.
75. Jameson, G. B., Molinaro, F. S., Ibers, J. A., Collman, J. P., Brauman, J. I., Rose, E., and Suslick, K. S. (1980) Models for the active site of oxygen-binding hemoproteins. Dioxygen binding properties and the structures of (2-methylimidazole)-*meso*-tetra-(α,α,α,α-o-pivalamidophenyl)porphyrinatoiron(II)-ethanol and its dioxygen adduct, *J. Am. Chem. Soc. 102*, 3224−3237.
76. Scherlis, D. A., and Estrin, D. A. (2001) Hydrogen bonding and O_2 affinity of hemoglobins, *J. Am. Chem. Soc. 123*, 8436−8437.

BI036273Z